



CONTINUOUS ADJOINT–BASED AEROACOUSTIC SHAPE OPTIMIZATION OF AN AERO–ENGINE INTAKE

Morteza Monfaredi
Dr. Varvara Asouti
Dr. Xenofon Trompoukis
Dr. Konstantinos Tsiakas
Prof. Kyriakos C. Giannakoglou

EUROGEN 2021

28-30 June 2021, Athens, Greece

14th International Conference on Evolutionary and Deterministic Methods for Design, Optimization and Control



Outline

- The Hybrid Noise Prediction Tool
- Continuous Adjoint Formulation
- Verification, Comparison to an Analytical Solution
- The Aero-Engine case
- Conclusion



The Hybrid Noise Prediction Tool

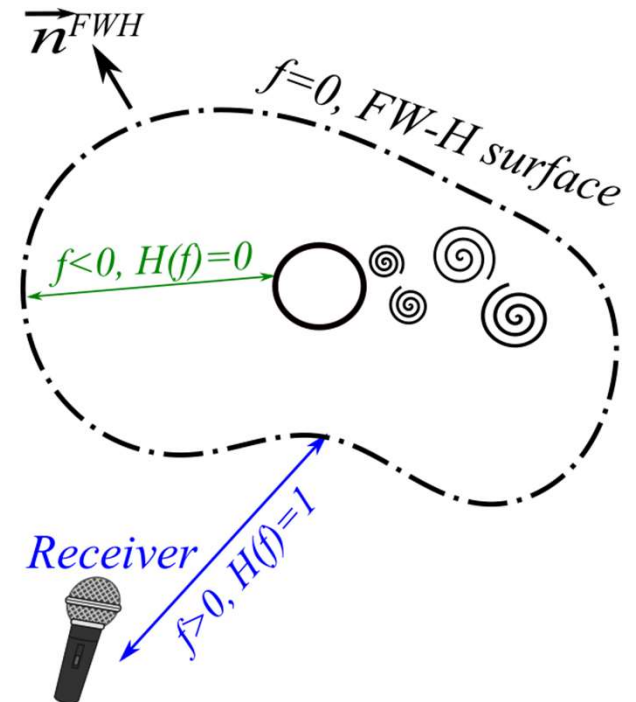
- Flow solution using in-house GPU-enabled software, PUMA.
 - RANS in a relative frame of reference (MRF).
- Acoustic propagation based on the Ffowcs Williams and Hawkins (FW-H) Analogy.
 - The FW-H integral in the frequency domain:

$$H(f)\hat{p}'(\vec{x}_r, \omega) = - \int_{f=0} i\omega \hat{Q}(\vec{x}_s, \omega) \hat{G}(\vec{x}_r, \vec{x}_s, \omega) ds - \int_{f=0} \hat{\mathcal{F}}_i(\vec{x}_s, \omega) \frac{\partial \hat{G}(\vec{x}_r, \vec{x}_s, \omega)}{\partial x_{s_i}} ds$$

$$Q(\vec{x}, t) = (\rho u_i - \rho_\infty u_{\infty i}) n_i^{\text{FWH}}$$

$$\mathcal{F}_i(\vec{x}, t) = [\rho(u_i - 2u_{\infty i})u_j + \rho_\infty u_{\infty i}u_{\infty j} + p\delta_{ij} - \tau_{ij}] n_j^{\text{FWH}}$$

$$\hat{G}(\vec{x}_r, \vec{x}_s, \omega) = -\frac{\exp(-ikr^+)}{4\pi r^*} \quad r^+ = \frac{1}{\beta^2}(r^* - \vec{M} \cdot \vec{r}), \quad r^* = \sqrt{(\vec{M} \cdot \vec{r})^2 + |\vec{r}|^2 \beta^2}, \quad \vec{r} = \vec{x}_r - \vec{x}_s, \quad \vec{M} = \frac{\vec{u}_\infty}{c_\infty}$$





Continuous Adjoint Formulation

The objective function is the total energy contained in the spectrum of the sound pressure:

$$J = \frac{1}{N_r} \sum_{a=1}^{N_r} \int_{\omega} |\hat{p}'(\vec{x}_{ra}, \omega)| d\omega \quad |\hat{p}'| = \sqrt{\hat{p}'_{\text{Re}}^2 + \hat{p}'_{\text{Im}}^2}$$

Design variables b_i are updated with a steepest descent algorithm $b_i^{\text{new}} = b_i^{\text{old}} - \eta \frac{\delta J}{\delta b_i}$

Lagrangian: $J_{aug} = J + \int_{T_s} \int_{\Omega} \Psi_n R_n d\Omega dt$ Differentiation w.r.t. b_i $\frac{\delta J_{Aug}}{\delta b_i} = \frac{\delta J}{\delta b_i} + \int_{T_s} \int_{\Omega} \Psi_n \frac{\delta R_n}{\delta b_i} d\Omega dt$

$$\frac{\delta J}{\delta b_i} = \int_{T_s} \int_{\Omega} \textcircled{FAE_n} \frac{\delta U_n}{\delta b_i} d\Omega dt + \int_{T_s} \int_{S_w} \textcircled{ABC_r} \frac{\delta U_n}{\delta b_i} dS dt + \int_{T_s} \int_{\Omega} \textcircled{SD_{nl}^2} \frac{\partial}{\partial x_m} \left(\frac{\delta x_l}{\delta b_i} \right) d\Omega dt + \int_{T_s} \int_{\Omega} \textcircled{SD^s} \frac{\delta x_l}{\delta b_i} dS dt$$

Field Adjoint
Equations

Adjoint Boundary
Conditions

Sensitivity
Derivative

Sensitivity
Derivative



Field Adjoint Equations & Sensitivity Derivatives

$$\text{FAE: } -\frac{\partial \Psi_m}{\partial t} - \frac{\partial f_{nk}^{inv}}{\partial U_m} \frac{\partial \Psi_n}{\partial x_k} - \left(\frac{\partial \tau_{qk}^{adj}}{\partial x_k} - \frac{\partial \Psi_5}{\partial x_k} \tau_{kq} \right) \frac{\partial u_q}{\partial U_m} - \frac{\partial q_k^{adj}}{\partial x_k} \frac{\partial T}{\partial U_m} - \frac{\partial J}{\partial U_m} \delta(f) = 0$$

$$\text{ABC: } \Psi_{m+1} n_m = 0 \quad \text{and} \quad q_k^{adj} n_k = 0 \quad \text{on solid surfaces.}$$

Sensitivity derivatives:

$$\begin{aligned} \frac{\delta J}{\delta b_e} = & - \int_{T_s} \int_{\Omega} \left[\Psi_n \left(\frac{\partial f_{nk}^{inv}}{\partial x_i} - \frac{\partial f_{nk}^{vis}}{\partial x_i} \right) + \tau_{mk}^{adj} \frac{\partial u_m}{\partial x_i} + q_k^{adj} \frac{\partial T}{\partial x_i} \right] \frac{\partial}{\partial x_k} \left(\frac{\delta x_i}{\delta b_e} \right) d\Omega dt \\ & + \int_{T_s} \int_S (p \Psi_{k+1} - \Psi_n f_{nk}^{inv} + \Psi_5 q_k + \Psi_5 u_m \tau_{mk}) \frac{\delta n_k}{\delta b_e} dS dt \end{aligned}$$

$$\tau_{mk}^{adj} = (\mu + \mu_t) \left[\frac{\partial \Psi_{m+1}}{\partial x_k} + \frac{\partial \Psi_{k+1}}{\partial x_m} + \frac{\partial \Psi_5}{\partial x_m} u_k + \frac{\partial \Psi_5}{\partial x_k} u_m - \frac{2}{3} \delta_{mk} \left(\frac{\partial \Psi_{l+1}}{\partial x_l} + \frac{\partial \Psi_5}{\partial x_l} u_l \right) \right]$$

$$q_k^{adj} = C_p \left(\frac{\mu}{Pr} + \frac{\mu_t}{Pr_t} \right) \frac{\partial \Psi_5}{\partial x_k}$$

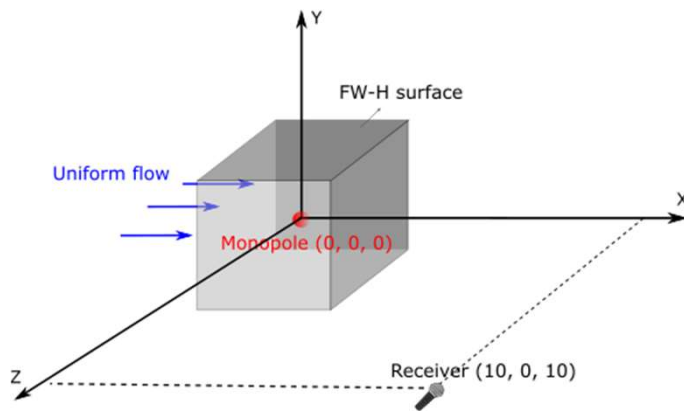


Verification w.r.t. Analytical Solution

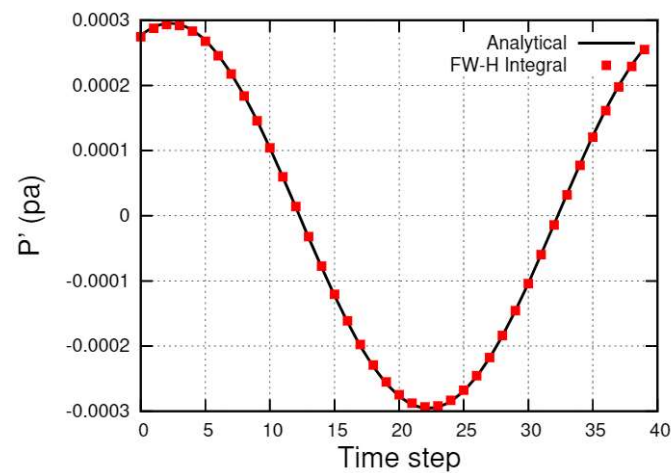
Perturbation field from a monopole sound source in flow $p' = -\rho_0 \left(\frac{\partial \phi}{\partial t} + v_{\infty 1} \frac{\partial \phi}{\partial x} \right)$, $v' = \nabla \phi$ and $\rho' = p'/c_0^2$

Velocity potential of monopole in flow for 3D $\phi(\vec{x}_r, \vec{x}_s, \omega) = A \exp(i\omega t) \frac{\exp(-ikr^+)}{4\pi r^*}$

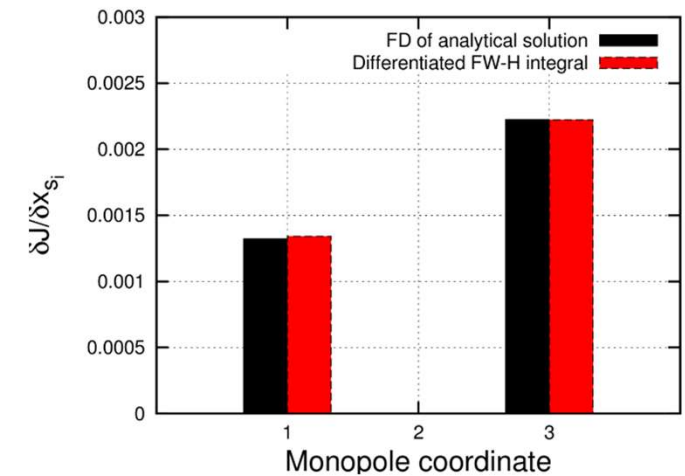
Verification of the FW-H implementation and differentiation



Pressure fluctuation at receiver location



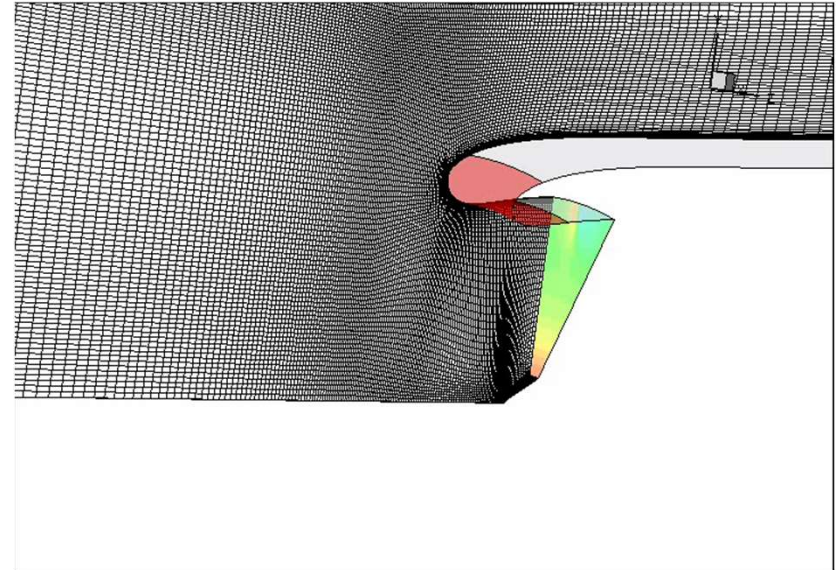
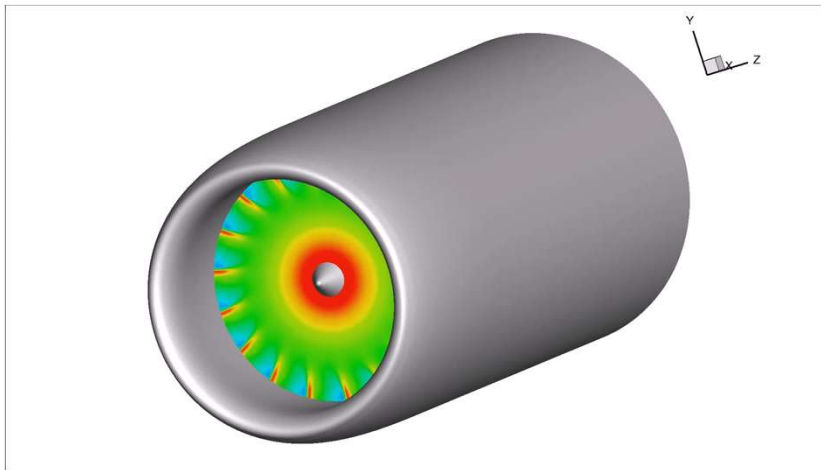
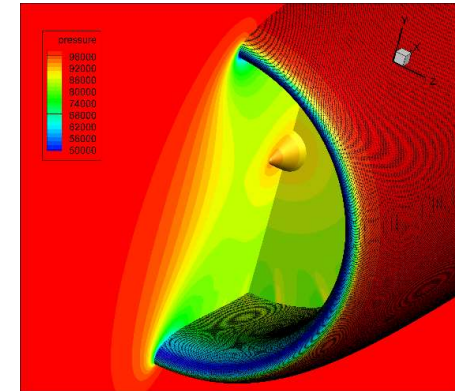
Derivatives w.r.t. monopole coordinates





The Aero-Engine Intake

- Generic intake geometry (scaled to match the Vital fan) by RR.
- Pressure distribution on the fan inlet provided by ISVR of the University of Southampton.
- S-A Turbulence model
- Single blade passage Mesh ~ 3.7M nodes on 100 meridional planes
- ~16 K nodes on FWH surface
- Flow and adjoint solved in a rotating frame of reference (steady).

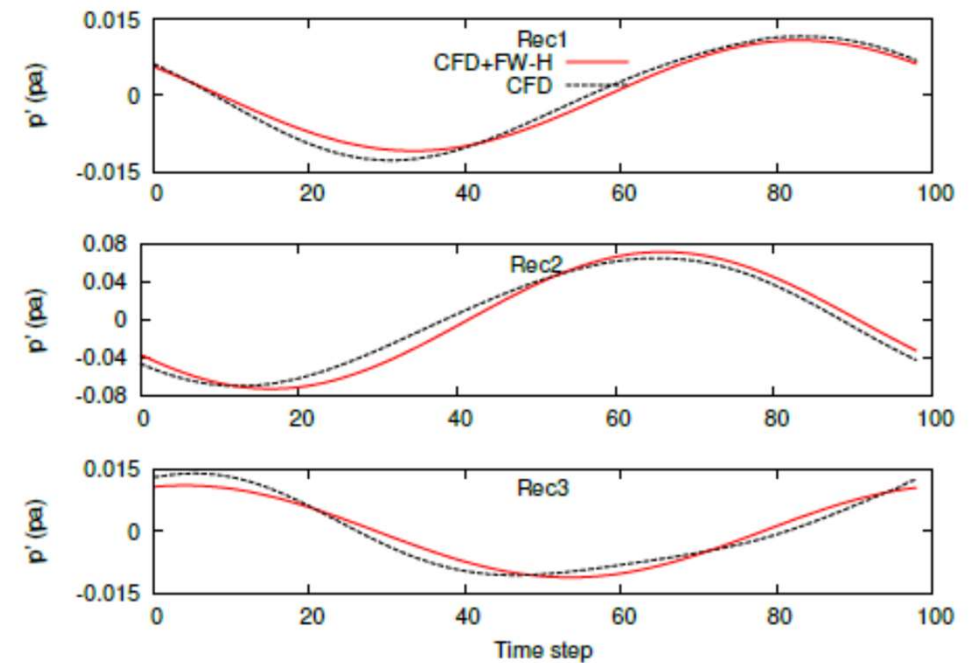
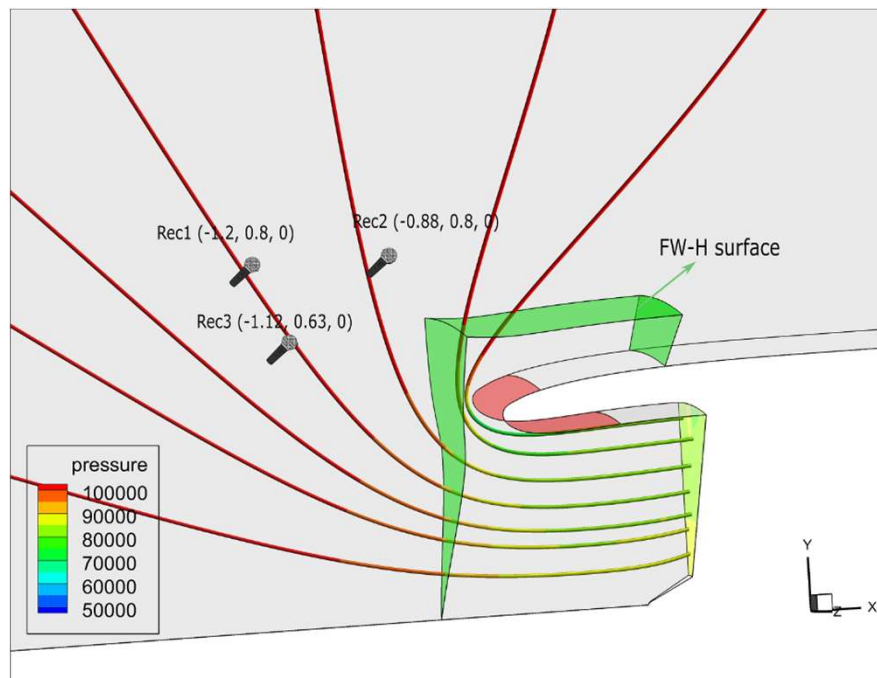




Optimization of a Turbofan Intake

Comparison between hybrid method and (U)RANS

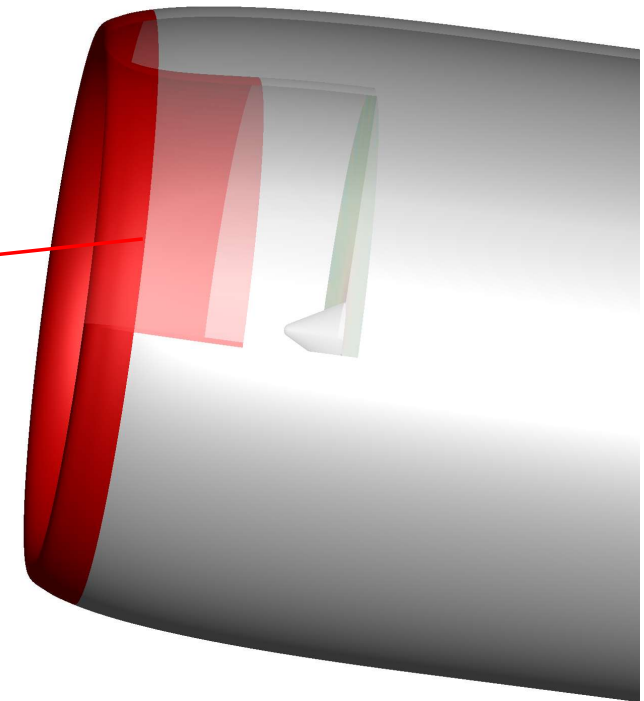
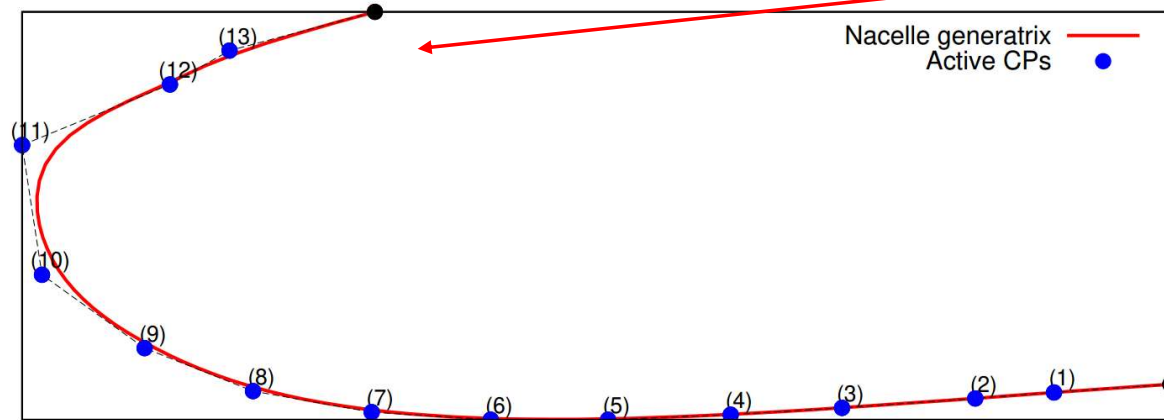
- Unsteady data on the FW-H surface extracted by performing rotation.





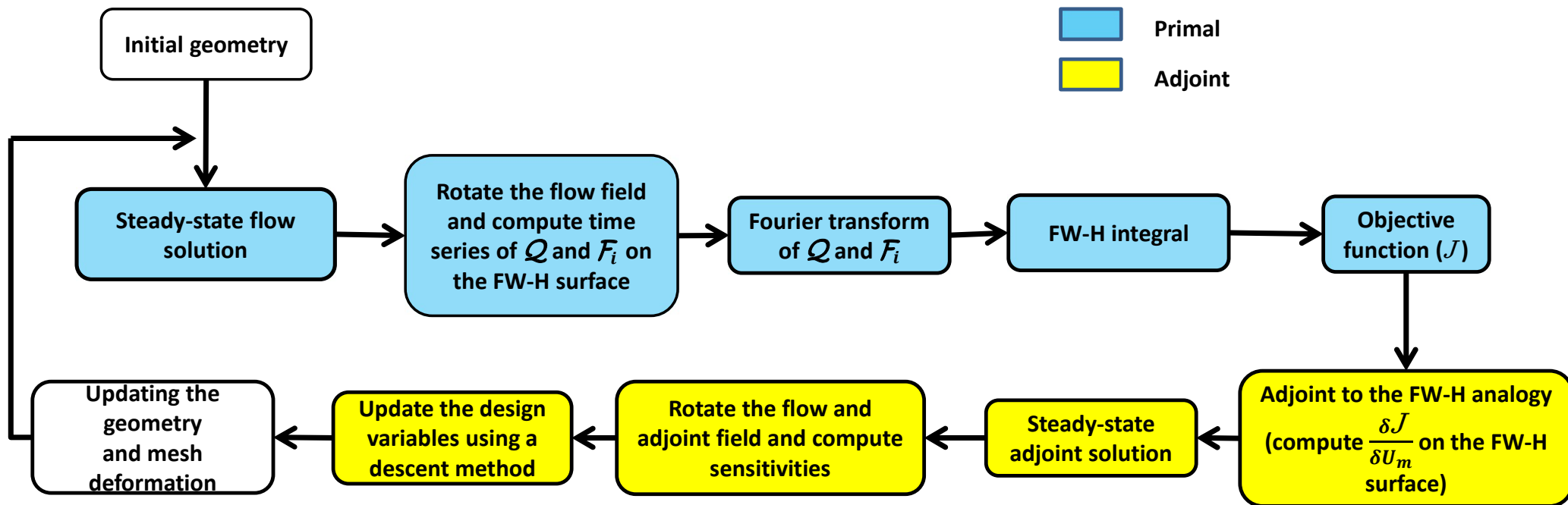
Optimization of a Turbofan Intake

- Generatrix parameterized using 15 control points.
- 13 are allowed to vary in the axial and radial direction; 26 DVs.
- Axisymmetric distribution of receivers to achieve periodic adjoint field.
- Steady adjoint.
- Rotation of the adjoint and flow field to compute sensitivities.
- Noise objective defined at the blade passing frequency.



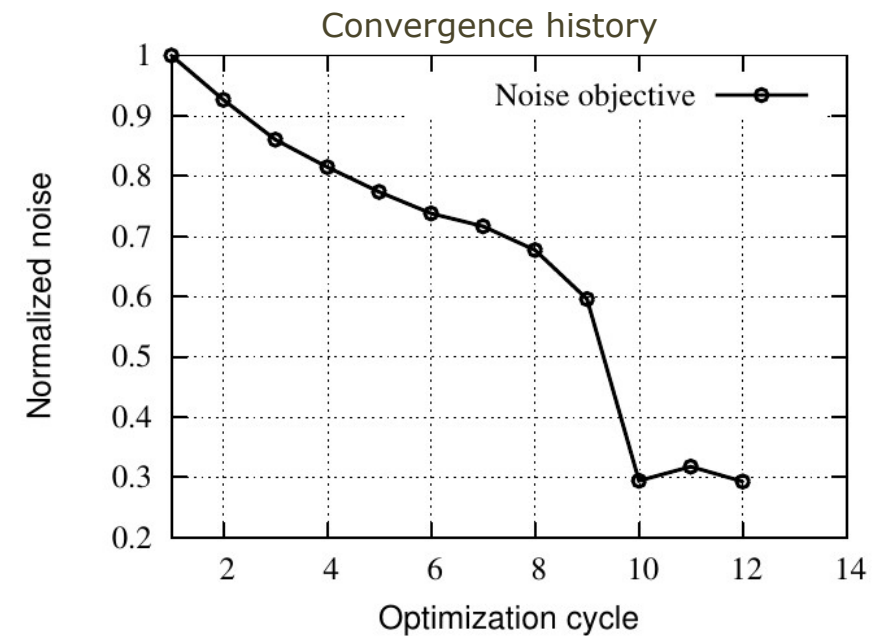
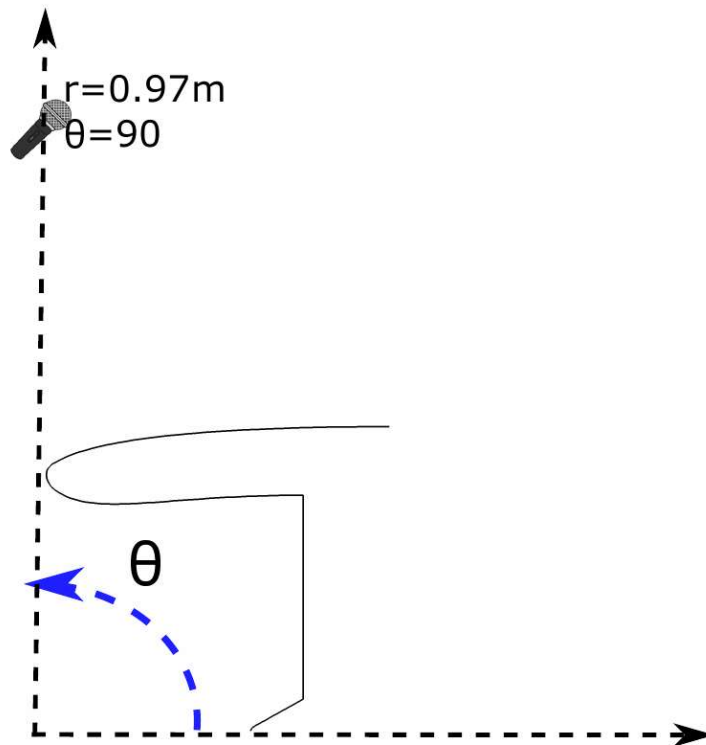


Aeroacoustic Shape Optimization Flowchart





Optimization for a Single Circumferential Row of Receivers

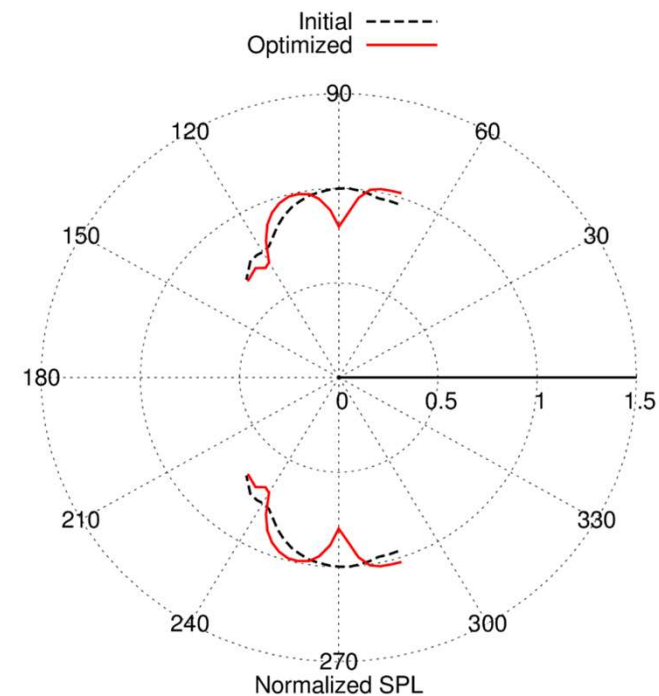
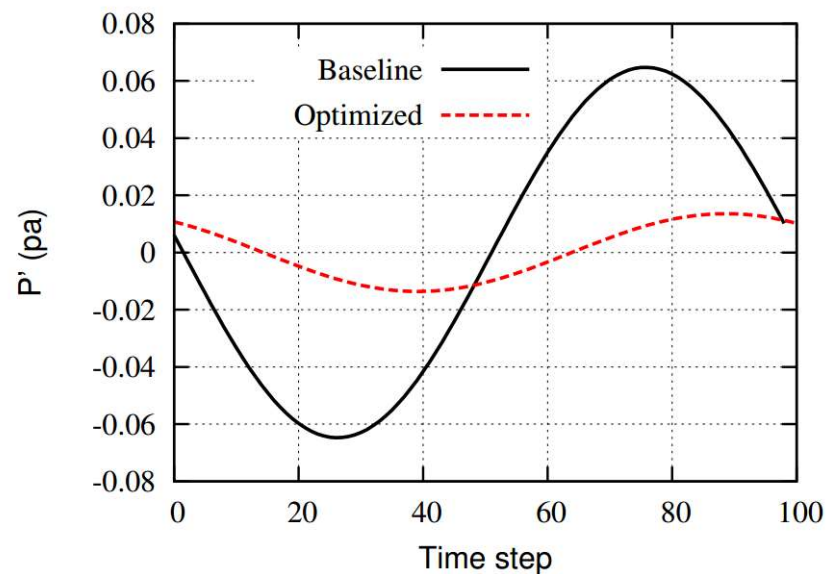


~70% reduction in the noise objective



Optimization for a Single Circumferential Row of Receivers

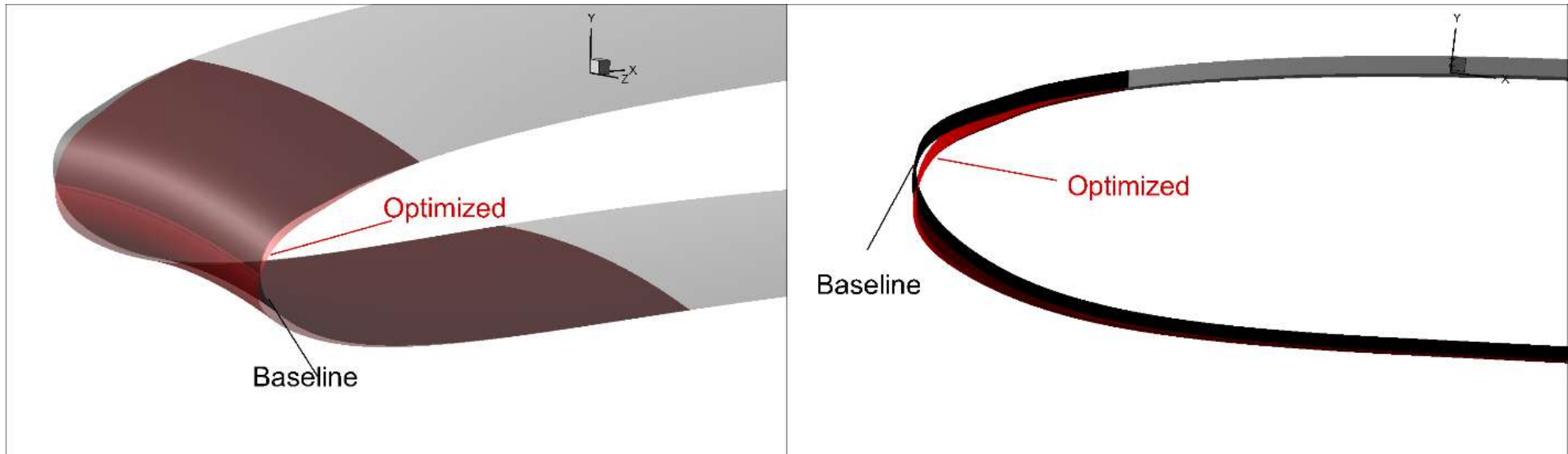
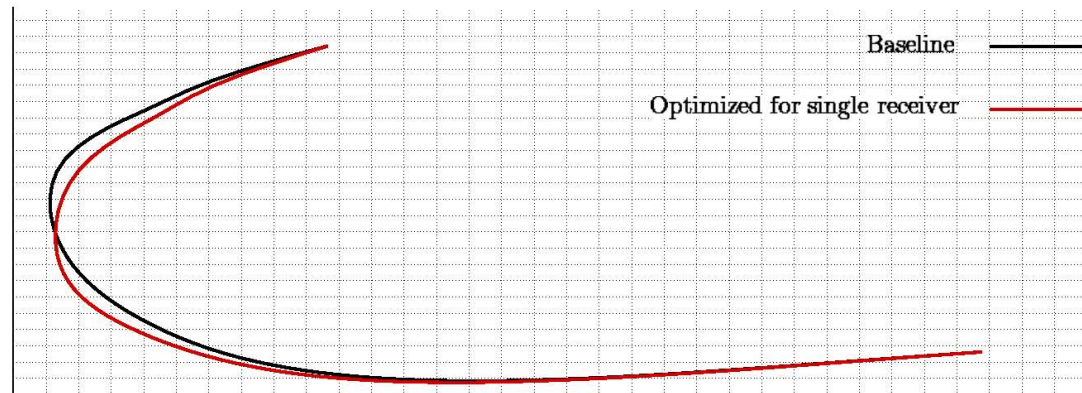
- Reduced amplitude of sound pressure.
- Slightly worse aerodynamic performance. $\sim 0.6\%$ increase in P_t loss.
- Directional noise reduction.



Max reduction ~ 10 dB

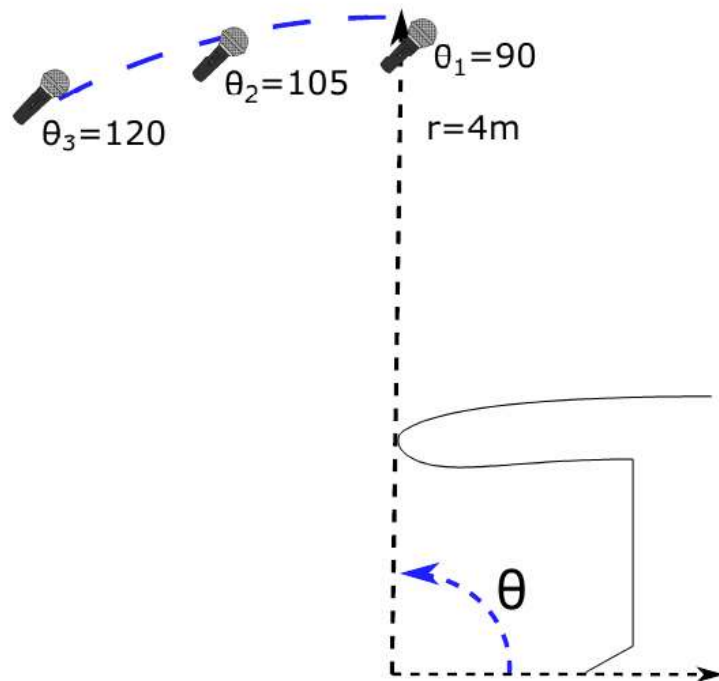


Optimization for a Single Circumferential Row of Receivers

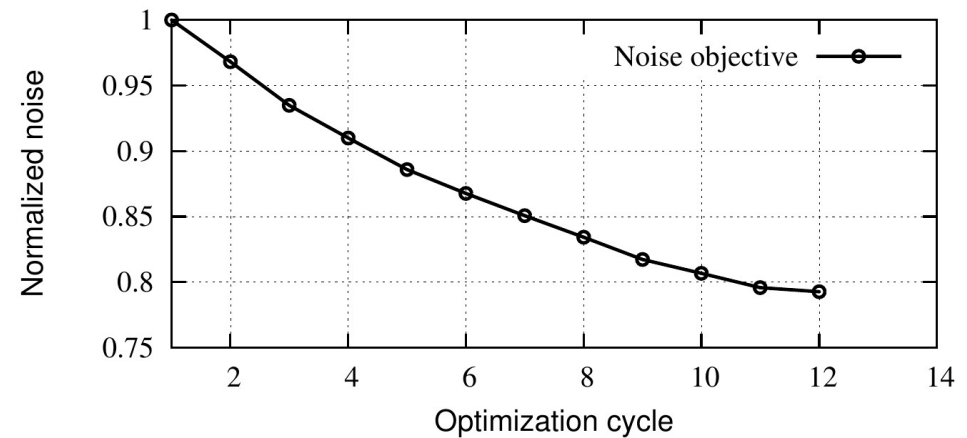




Optimization for Three Circumferential Rows of Receivers



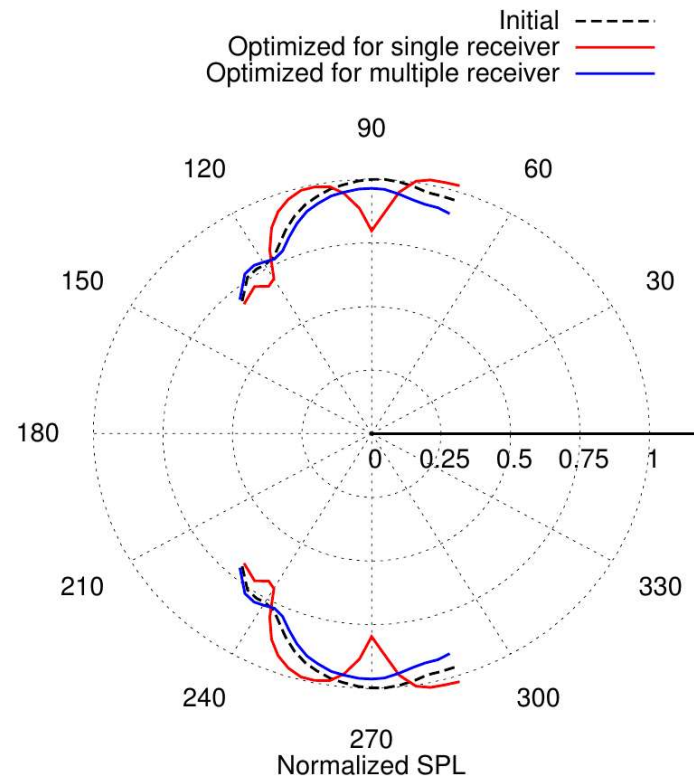
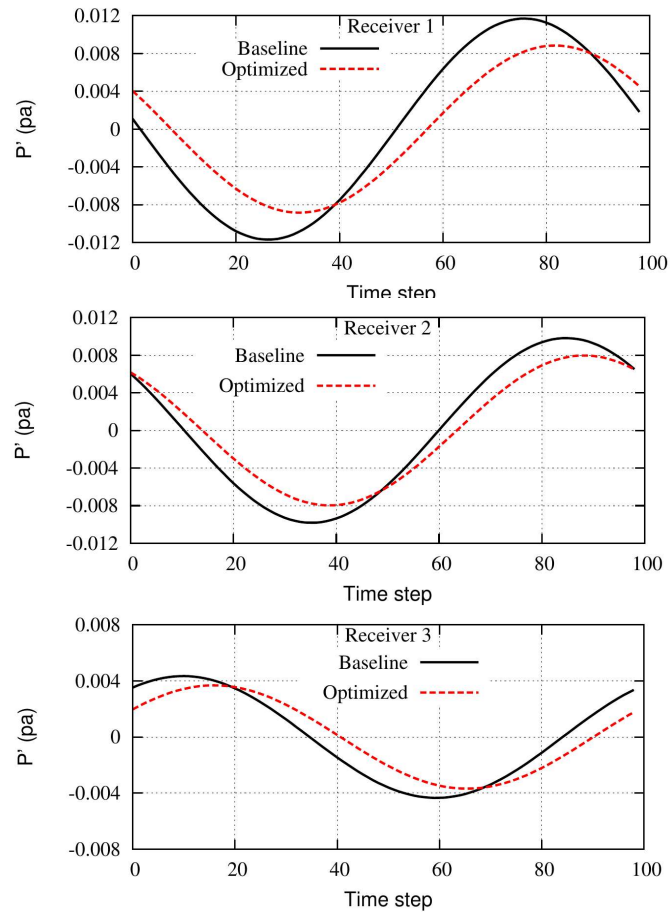
Convergence history



~20% reduction in the noise objective
Better ($\sim 0.12\%$) aerodynamic performance



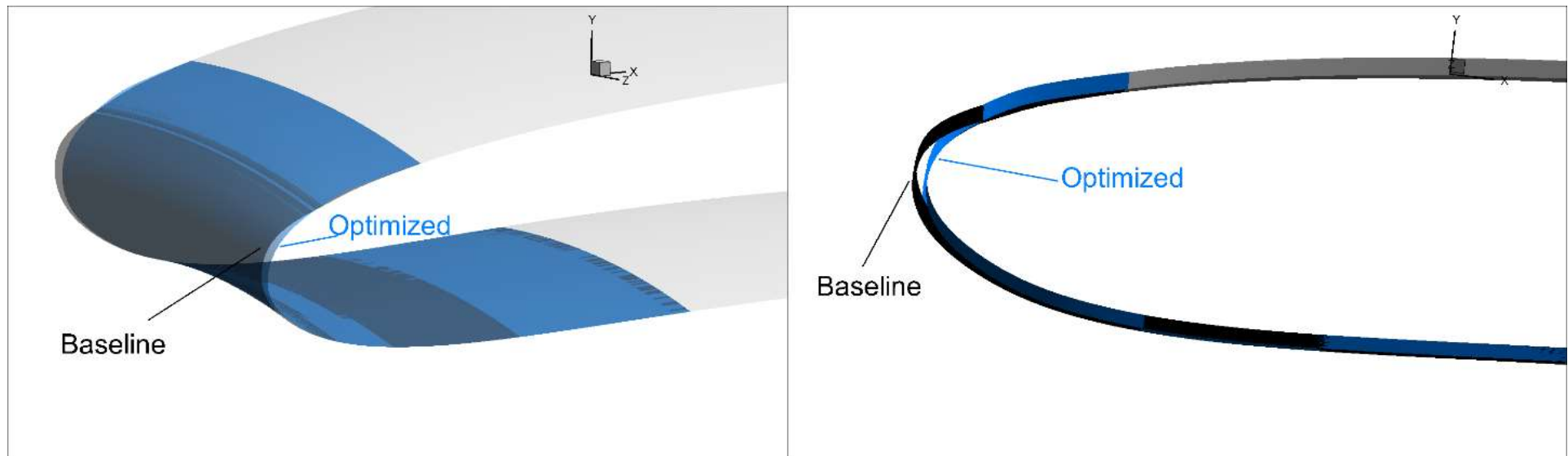
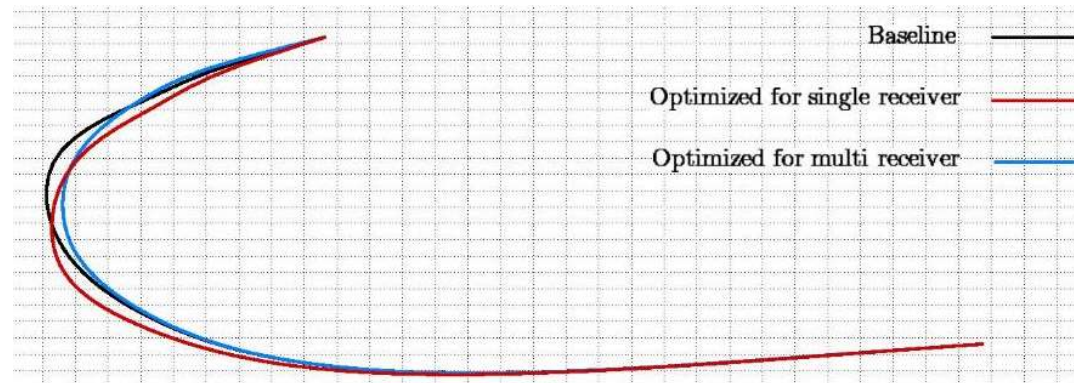
Optimization for Three Circumferential Rows of Receivers



Max reduction ~2.5 dB



Optimization for Three Circumferential Rows of Receivers





Conclusion

- A previous implementation of the permeable version of the FW-H analogy in the frequency domain, for 2D problems, is extended and verified in 3D.
- Differentiation of the FW-H analogy is verified by comparison to analytical solution of sound field from a monopole source.
- Overall optimization tool runs on NVIDIA GPUs.
- Flow and adjoint are solved in a rotation frame of reference (steady).
- The unsteady fields of flow and adjoint solutions are achieved by rotation of the steady fields.
- The previous step overcomes the problems of large memory requirement and long solution time.
- Aeroacoustic shape optimization performed for both single and multiple receiver locations.



This project has received funding from the European Union's Horizon 2020 research and innovation programme under grant agreement N° 769025.



www.madeleine-project.eu
www.linkedin.com/company/madeleine-project/